CGU HS Committee on River Ice Processes and the Environment
19th Workshop on the Hydraulics of Ice Covered Rivers
Whitehorse, Yukon, Canada, July 9-12, 2017.

Anchor ice effects on the hyporheic environment in a hydropeaking stream

Jennifer Nafziger[1], Tae Chung[1], and Yuntong She[1]
[1]*Department of Civil and Environmental Engineering, University of Alberta,*
7-203 Donadeo Innovation Centre for Engineering, Edmonton, Alberta, T6G 1H9
jnafzige@ualberta.ca
thchung@ualberta.ca
yshe@ualberta.ca

The hyporheic zone, where surface water and groundwater actively interact, exists beneath and alongside many river beds. It is important habitat for the fish species whose embryos incubate there over the winter, a season that represents a "bottleneck" in aquatic species survival. Dissolved oxygen and water temperature are important controls on the development and survival of these embryos. Extensive research has been conducted to study the hydrological and ecological processes of the hyporheic zone. However, very little is known about the impact that river ice may have on this zone and on the exchange between surface and hyporheic waters. This paper presents observations of dissolved oxygen and temperature in the hyporheic zone during several anchor ice formation and release events on the Kananaskis River in Alberta, Canada.

1 Introduction

The hyporheic zone is that portion of sediment beneath and alongside a stream where surface water from the stream and shallow groundwater mix. Different definitions of the hyporheic zone exist, but a common feature is the two-way exchange of water in the hyporheic zone, where water is transported back and forth between the sediments and the surface water over scales of centimeters to tens of meters (Goosef, 2010). Many biogeochemical processes occur in the hyporheic zone and it has been metaphorically referred to as "a river's liver" because of the nutrient cycling that can occur there (Fischer et al., 2005). The dissolved oxygen (DO) content and temperature of hyporheic water may be particularly important for the embryos of many autumn-spawning salmonid fishes which incubate in the hyporheic zone over the winter season (e.g. Malcolm et al., 2003). The exchange of water across the stream bed is driven by the pressure distribution on the bed and is therefore influenced by stream stage and the presence of stream and bed features (Boano et al., 2014). For example, Casas-Mulet et al. (2015) demonstrated that hyporheic processes are sensitive to stage changes due to hydropeaking and Hester et al. (2009) and Sawyer et al. (2011, 2012) demonstrated how weirs and channel-spanning logs can influence hyporheic water and heat flux.

Given how the formation of anchor ice changes both channel features and stream stage (e.g. Nafziger et al., 2017), it is likely to affect the water in the hyporheic zone. However, relatively few researchers have investigated hyporheic exchange in the context of ice-affected streams. Kempema and Konrad (2004) observed an increase in the temperature of hyporheic waters when anchor ice accumulations diverted channel flow and caused a decrease in stream stage. Cardenas and Gooseff (2008) simulated the effect of an ice cover on hyporheic exchange for a hypothetical case. Weber et al. (2013) observed reduced groundwater discharge to a stream during the stage rise associated with surface ice formation events. In addition, hyporheic or groundwater process may in turn influence anchor ice processes. Kempema and Konrad (2004) noted that hyporheic flow paths may influence the distribution of anchor ice on a streambed, and that anchor ice and hyporheic heat flux may affect each other. Tremblay et al. (2013) noted that their laboratory-simulated anchor ice did not release without water flowing in a gravel layer under the ice, which may indicate the importance of hyporheic flow on the release of anchor ice. The heat budget model of Turcotte et al. (2013) implied that the influence of anchor ice on groundwater exchange may result in self-sustaining anchor ice dams. Finally, a recent comprehensive review of hyporheic processes by Boano et al. (2014) assessed many drivers of hyporheic exchange but was silent on how river ice may alter hyporheic processes, demonstrating the need for more research in this area.

The purpose of this paper is two-fold: 1) present observations of how hyporheic DO and water temperature responded to anchor ice formation and release; and 2) present preliminary hypotheses of how and why anchor ice may affect hyporheic exchange.

2 Study Sites and Methods

Ice processes and hyporheic exchange was studied at two sites on the Kanansaksis River in the Rocky Mountains of Alberta, Canada (Figure 1). This section of the Kananaskis River lies downstream of the Pocaterra Dam, and experiences extreme daily discharge changes from < ~0.5 m^3/s to ~24 m^3/s as a result of hydropeaking for electricity generation. The river is a tortuously meandering river with a gravel and cobble bed and frequent multi-channel sections (Buehler, 2013) with an average slope of 0.5%. The reach at Site 1 (Figure 2a) is located 14.6 km downstream of the Pocaterra Dam and consists of a ~20 m wide single channel. The water depths ranged from a few cm to 60 cm at low flow and with an average daily increase in depth due to hydropeaking of approximately 55 cm during ice-free conditions. This site is known to experience occasional anchor ice events (Emmer et al., 2013), an example of which is shown in Figure 2b. Site 2, (Figure 3a) located 37.5 km downstream of the Pocaterra dam, is approximately 40 m wide including a large 20 m wide mid-channel bar, which is exposed at low flow. Measurements were taken on the right side of this bar where flow depths and velocities were smaller than on the left side. Water depths ranged from a few cm to 80 cm at low flow with an average daily increase in depth due to hydropeaking of approximately 45 cm during ice-free conditions. This site has been observed to experience a floating surface ice cover, anchor ice, and a type of layered, hardened anchor ice, which forms during the repeated flooding and draining of bed surfaces during hydropeaking (Emmer et al., 2013), an example of which is shown in Figure 3b.

Ice processes, stream stage, air temperature, as well as water temperature and DO in the surface water and in the hyporheic zone were observed at regular intervals from late October 2013 to late April 2014. Ice processes were observed half-hourly during daylight hours using tree mounted time-lapse cameras (Reconyx RapidFire). DO and temperature were measured every 15 minutes using submersible optical DO sensors and dataloggers (Onset HOBO U26, DO accuracy: 0.2 to 0.5 mg/L, temperature accuracy: 0.2 °C). The DO sensors were calibrated at 100% and 0% saturation before deployment and after they were retrieved. Stream stage was measured every 10 minutes using submersible, self-contained pressure transducers and dataloggers (Schlumberger Diver model 601, accuracy: 0.5 cmH_2O). The pressure data were corrected to eliminate the effects of atmospheric pressure changes using data from barometric pressure dataloggers (Schlumberger Diver model DI500, accuracy: 0.5 cmH_2O) installed ~4 m above stream level at each site. Surface water sensors were installed in perforated heavy steel cases installed at the bed surface. Hyporheic zone sensors were installed 30 cm below the bed surface in a cased hole driven with a custom-made driver similar to that used by Casas-Mulet et al. (2015). After each hyporheic zone sensor was placed at the correct depth, the casing was removed, leaving only the sensor in the substrate. Finally, hourly air temperature measurements were provided by the University of Calgary's Biogeoscience Institute, who operate a weather station at the nearby Barrier Lake Field Station (Figure 1).

Percent saturation of DO (% sat.) was calculated as a proportion of the oxygen solubility (i.e. concentration at 100% saturation) at the observed water temperature and atmospheric pressure. Oxygen solubility was calculated using the method of Benson and Krause (1980 and

1984) as implemented in the DOTABLES v3.5 program (United States Geological Survey, 2013) using the barometric pressures measured at each site, water temperatures measured by the DO measuring device and a salinity of 0 % for fresh water.

3 Results

Dissolved oxygen in the surface (DO_s) and hyporheic water (DO_h), stream stage, ice conditions, temperature of the surface (T_{ws}) and hyporheic (T_{wh}) water are shown in Figures 4 to 8 for five example time periods (Table 1), chosen to illustrate possible ice effects on the hyporheic zone. The one or two most prevalent ice conditions (in terms of channel area covered) are shown in panel d) of these figures; the ice condition that was most prevalent is shown as "primary", and the other as "secondary". If only one ice condition was present, it is shown in both rows. Frequently, ice conditions could not be observed due to darkness, camera fogging, or the presence of glare or ripples obscuring the view of anchor ice; these periods are shown in panel d) as "no data". These figures also show the air temperature (T_a) and stream discharge at the dam (Q_d). The discharge shown has been lagged by the wave travel time to the sites (2.9 hrs. for Site 1, 7.75 hrs. for Site 2), which was determined by matching the discharge wave to the observed water level wave under autumn ice-free conditions.

3.1 Time Period 1: Open Water Hydropeaking Pulse at Site 1

Time Period 1 (Figure 4) was an ice-free period at Site 1 that included one hydropeaking pulse (Q_d, Figure 4f), chosen to illustrate the effects of hydropeaking on the measured parameters. During this period, DO_s was fairly constant ~11.0 mg/L (95% sat.) before the hypropeaking pulse and increased slightly to ~11.5 mg/L (97 % sat.) at the time the pulse arrived (Figure 4b). The DO_h was lower than the DO_s but experienced a larger increase from ~7.5 mg/L (64 % sat.) to 9.4 mg/L (80% sat.) with the DO increase lagging the stage increase by approximately 1 hr. The DO_h decreased in response to the stage decrease with a lag of approximately 30 minutes, suggesting a faster hyporheic response to falling stages than to rising stages. The T_{ws} was two-peaked (Figure 4e); the first peak corresponded to the afternoon when heating from shortwave radiation was expected to have been greatest, and the second peak corresponded to the hydropeaking pulse. The T_{wh} decreased slightly during the hydropeaking pulse, and continued to decrease after the pulse had passed.

3.2 Time Period 2 and 3: Multi-Day Anchor Ice Events at Site 1

Time Period 2 (Figure 5) represents a multi-day anchor ice event at Site 1. During this event anchor ice formed overnight Dec 3–4 and persisted through the daylight, low-water periods until it released overnight Dec 10–11. The continued presence of the anchor ice during the night-time high-flow hydropeaking events could not be confirmed, but is considered likely because T_{ws} remained at ~0 °C until Dec10 (Figure 5e). The stage (Figure 5c) peaked every night with the hydropeaking pulses (Figure 5f), and the stage of the "valleys" between the peaks were higher than during open water (dashed grey horizontal line on Figure 5c) and increased because of the presence and growth of anchor ice in the channel.

DO_s, DO_h, and T_{wh} changed when anchor ice was present in the channel (Figures 5b and 5e). From Dec 5 to 7 the DO_s gradually decreased to 0 mg/L and then abruptly increased on Dec10 as the anchor ice released. At the same time, the DO_h increased from ~7.5 mg/L (65% sat.) to ~11.5 mg/L (85% sat.) and then quickly decreased on Dec 10. The T_{ws} was fairly constant at ~0 °C, while the T_{wh} decreased from 1.2 °C to ~0.1°C during the event; both T_{ws} and T_{wh} increased near the end of the anchor ice event, with T_{ws} increasing to 0.4 °C as the anchor ice released. During Time Period 3 at Site 1, a similar pattern was observed whereby the DO_s decreased and the DO_h increased during a separate multi-day anchor ice event (Figure 6). However, during Time Period 3, the DO_s increased dramatically with the hydropeaking pulse on Jan 5-6 before decreasing gradually again the next day.

3.3 Time Period 4: Anchor Ice Event at Site 2

During Time Period 4 (Figure 7) anchor ice formed at Site 2 overnight Nov 18-19 during snowfall and cold air temperatures. During the daily high flow periods, layers of anchor ice also formed on the mid-channel bar at the site, which were later exposed at low flow. The end of this anchor ice event at the location of the sensor is uncertain because water surface conditions obscured view of the anchor ice; however observations from other cameras at this site, which were focused on the opposite side of the bar, indicate that the event ended on the afternoon of Nov 23 when the air temperature (Figure 7g) climbed to above freezing. During this event, the DO_s was fairly constant at ~12 mg/L (95 % sat.) while the DO_h increased slightly overnight Nov 19-20 from 11.6 mg/L (91 % sat.) to 12.3 mg/L (97 % sat.) The T_{ws} remained ~0 °C while T_{wh} decreased from ~0.1 °C to ~0 °C at the start of the event.

3.4 Time Period 5: Low DO_h Period Under Surface Ice Cover at Site 2

During Time Period 5 an extended period of low DO_h was observed at Site 2 when the site was covered with surface ice, with occasional periods of overflow. In the month prior to Time Period 5, grounded layered anchor ice formed on the mid-channel bar and anchor ice formation caused the majority of the flow at Site 2 to be diverted to the left side of the ice-covered bar, opposite to where the sensors were installed, as evidenced by the very small (~5-10 cm) stage change interval during hydropeaking. During this time of low flow on the right side of the bar, a surface ice cover formed on both sides of the channel and DO_s and DO_h remained relatively high (10-12 mg/L, 79-94 % sat.). Starting Feb 4, the hydropeaking stage interval dramatically increased (to 75-100 cm) and the DO_h increased (with daily oscillations) until Feb 7. After Feb 7, DO_h started to gradually decrease reaching a minimum of 2.05 mg/L on Mar 1. After Feb 12 the hydropeaking stage interval decreased to ~25 cm. After several weeks of low DO_h, the DO_h then increased dramatically over Mar 16-18 to ~12 mg/L (94 % sat.). Throughout Time Period 5 both T_{ws} and T_{wh} were ~0 °C.

4 Discussion

A few general trends of how DO_h and T_{wh} changed in response to stage changes were observed. When hydropeaking caused a stage increase during the autumn ice-free period, a corresponding increase in DO_h and decrease in T_{wh} were observed. Similarly, stage increases

caused by anchor ice growth also resulted in an observed increase in DO_h and T_{wh}. This suggests that higher stage due to hydropeaking or anchor ice forced high-DO and low-temperature stream water into the hyporheic zone. It is interesting that the changes in DO_h during the anchor ice events in Time Periods 2 and 3 were greater than the change of DO_h during typical ice-free hydropeaking pulses (e.g. Time Period 1) even though the stage change due to anchor ice (~5 to 40 cm) was smaller than the stage change due to hydropeaking (~55 cm) at Site 1. This may be the result of the response time of the hyporheic zone to changes in stage—the hyporheic zone at Site 1 appears to respond more quickly to decreases in stage than to increases (i.e. DO observed during Time Period 1). Therefore, the more prolonged stage increases during anchor ice events, which may last for several days, may allow for a greater fraction of surface water to enter the hyporheic zone compared to the relatively short stage increases (typically 8 to 12 hrs in duration) due to hydropeaking.

The low DO_s observed during the anchor ice events at Site 1 (Time Periods 2 and 3) could be attributed the accumulation of ice on the DO sensor. The effect of ice accumulation on DO sensor readings is not known, and should be tested. However, the gradual decrease and abrupt increase in DO_s (see Figure 5c and 6c) is consistent with what may be expected if anchor ice collected on the DO sensor, causing a decrease in DO readings, and then released quickly. This may explain the lower DO_s observed during anchor ice events at Site 1 (i.e. Time Periods 2 and 3). In addition, the abrupt rise in DO_h on Jan 5 during Time Period 3 may be the result of a partial release of the ice on the sensor during the hydropeaking pulse on that day.

What caused the dramatic and prolonged decrease in DO_h during Time Period 5 at Site 2 is not known. One possibility is that ice started to grow thermally on the DO sensor in the subsurface, perhaps after very cold water was transported to the hyporheic zone when the stage increased in early February. However, it may be unlikely that ice would form on the DO_h sensor and not the DO_s sensor, given that they are located ~3 m apart. Another possibility is that ice formation changed the surface flow patterns such that the fraction of low-DO groundwater increased in the hyporheic zone. However, this is not possible to verify given the sparse distribution of sensors and the presence of a surface ice cover that obscured view of the flow patterns.

5 Conceptual Models of the Effects of Anchor Ice on Hyporheic Exchange

Based on the observations presented in this paper and on the observations in the literature of the effects of channel features on hyporheic exchange, three conceptual models of how anchor ice may affect the hyporheic zone were developed. These models assume typical ice-affected stream conditions where the surface water has a higher DO and lower temperature than the shallow groundwater. The features of anchor ice that these models were developed to explore include: 1) the effect of an increase in stream stage due to anchor ice growth; 2) the effect of a contrast in hydraulic conductivity between the anchor ice accumulation and the stream bed material; 3) the effect of anchor ice growth on changing spatial flow patterns in a stream.

Figure 9 illustrates the possible hyporheic exchange flow paths for each anchor ice feature. Figure 9a shows hyporheic exchange in the case where anchor ice raises the water level, thereby forcing colder, higher-DO water into the hyporheic zone. This situation may result in anchor ice that is self-sustaining because anchor ice is surrounded in ~0 °C water above and below the accumulation. This may be similar to the anchor ice that was observed on the Kananaksis River, because DO_h increased when anchor ice was present (e.g. Time Periods 2, 3, and 4). Figure 9b shows an anchor ice accumulation that has a large contrast in hydraulic conductivity from the bed material. If the anchor ice has a higher hydraulic conductivity from the bed, the high DO surface water may preferentially flow through the anchor ice layer instead of being exchanged into the bed. If the anchor ice has a markedly lower hydraulic conductivity than the bed material, the ice may act as a barrier and prevent the mixing of surface and groundwater. Both of these situations may result in lower DO and higher temperature water being observed in the subsurface. Figure 9c shows a possible situation where changing flow paths caused by anchor ice causes a lower stage to occur than would have been observed under open water conditions. This may result in an increase in the groundwater fraction in the hyporheic zone, and therefore a lower DO_h may be observed (e.g. Time Period 5).

6 Conclusions and Recommendations

These observations indicate that anchor ice affected the hyporheic zone by increasing the DO and decreasing the water temperature there. This may be because the increased stage forced high DO surface water into the hyporheic zone. In addition, very low hyporheic DO was observed at Site 2 in February and March. This may be because of ice-induced changes in flow patterns, or because of ice buildup on the DO sensor, or because of another, unknown mechanism.

How ice buildup on the sensors affects DO readings should be examined further, to help explain the very low DO values observed during anchor ice events. This highlights the importance of testing any instruments to determine how they will respond in ice-affected environments, which may not be typical of the environments the instruments were designed for. Also, future studies should include a larger number of hyporheic observation locations to help elucidate what is happening in the event that flow pattern changes occur. An investigation into the hydraulic conductivity of anchor ice accumulations would also help understand how anchor ice may affect the hyporheic zone.

Finally, the conceptual models presented here may serve as hypotheses to aid in the design of future investigations of the effect of anchor ice on hyporheic processes.

Acknowledgments

This research was funded through grants and graduate scholarships from the Natural Sciences and Engineering Research Council of Canada through the HydroNet Strategic Network and Discovery Grant programs. This support is gratefully acknowledged. The authors would also like to thank TransAlta Corporation and the University of Calgary Biogeoscience Institute for providing the discharge and weather data and Michael Marchen for his assistance in the field.

References

Cardenas M.B., Gooseff M.N. 2008. Comparison of hyporheic exchange under covered and uncovered channels based on linked surface and groundwater flow simulations. Water Resources Research, 44(3).

Casas-Mulet, R., Alfredsen, K., Hamududu, B., Timalsina, N.P. 2015. The effects of hydropeaking on hyporheic interactions based on field experiments. Hydrological Processes, 29(6):1370-84.

Benson, B., Krause, D. 1980. The concentration and isotopic fractionation of gases dissolved in freshwater in equilibrium with the atmosphere 1: oxygen. Limnology and Oceanography, 25(4): 662-671.

Benson, B., Krause, D. 1984. The concentration and isotopic fractionation of oxygen dissolved in freshwater and seawater in equilibrium with the atmosphere. Limnology and Oceanography, 29(3):620-32.

Buehler, H. 2013. Impact of a hydropeaking dam on the Kananaskis River: changes in geomorphology, riparian ecology, and physical habitat. M.Sc. Thesis. University of British Columbia, Department of Geography, Vancouver, British Columbia.

Emmer, S., Nafziger, J., McFarlane, V., Loewen, M., Hicks, F. 2013. Winter Ice Processes of the Kananaskis River, Alberta. Poster. Proceedings of the 17th Workshop on River Ice, CGU-HS Committee of River Ice Processes and the Environment, Edmonton, Alberta.

Fischer, H., Kloep, F., Wilzcek, S., Pusch, M.T. 2005. A river's liver–microbial processes within the hyporheic zone of a large lowland river. Biogeochemistry, 76(2):349-71.

Gooseff, M.N., 2010. Defining hyporheic zones–advancing our conceptual and operational definitions of where stream water and groundwater meet. Geography Compass, 4(8):945-955.

Hester, E.T., Doyle, M.W., Poole, G.C. 2009. The influence of in-stream structures on summer water temperatures via induced hyporheic exchange. Limnology and Oceanography, 54(1):355-367.

Kempema, E.W., Konrad, S.K., 2004. Anchor ice and water exchange in the hyporheic zone. In 17th International Symposium on Ice, International Association of Hydraulic Engineering and Research, Saint-Petersburg, Russia.

Malcolm, I.A., Youngson, A.F., Soulsby, C. 2003. Survival of salmonid eggs in a degraded gravel-bed stream: effects of groundwater–surface water interactions. River Research and Applications, 19(4):303-16.

Nafziger, J. She, Y., Hicks, F. 2017. Anchor ice formation and release in small regulated and unregulated streams. Cold Regions Science and Technology, 141:66-77.

Sawyer, A.H., Cardenas, M.B., Buttles, J. 2011. Hyporheic exchange due to channel-spanning logs. Water Resources Research. 47(8).

Sawyer, A.H., Cardenas, M.B., Buttles, J. 2012. Hyporheic temperature dynamics and heat exchange near channel-spanning logs.Water Resources Research, 48(1).

Turcotte, B., Morse, B., Dubé, M., Anctil, F. 2013. Quantifying steep channel freezeup processes. Cold Regions Science and Technology, 94:21-36.

United States Geological Survey. 2013. DOTABLES (online software). Retrieved from http://water.usgs.gov/software/DOTABLES/

Weber, M.D., Booth, E.G., Loheide, S.P. 2013. Dynamic ice formation in channels as a driver for stream-aquifer interactions. Geophysical Research Letters, 40(13): 3408-3412.

Table 1. Time periods for which observations are presented.

Time Period #	Site	Dates	Description
1	Site 1	Nov 10 – 11, 2013	Hydropeaking during ice-free conditions
2	Site 1	Dec 4 – 13, 2013	Anchor ice event
3	Site 1	Jan 1 – 9, 2014	Anchor ice event
4	Site 2	Nov 19 – 24, 2013	Anchor ice event
5	Site 2	Feb 2 – Mar 19, 2014	Low DO_h period under surface ice cover

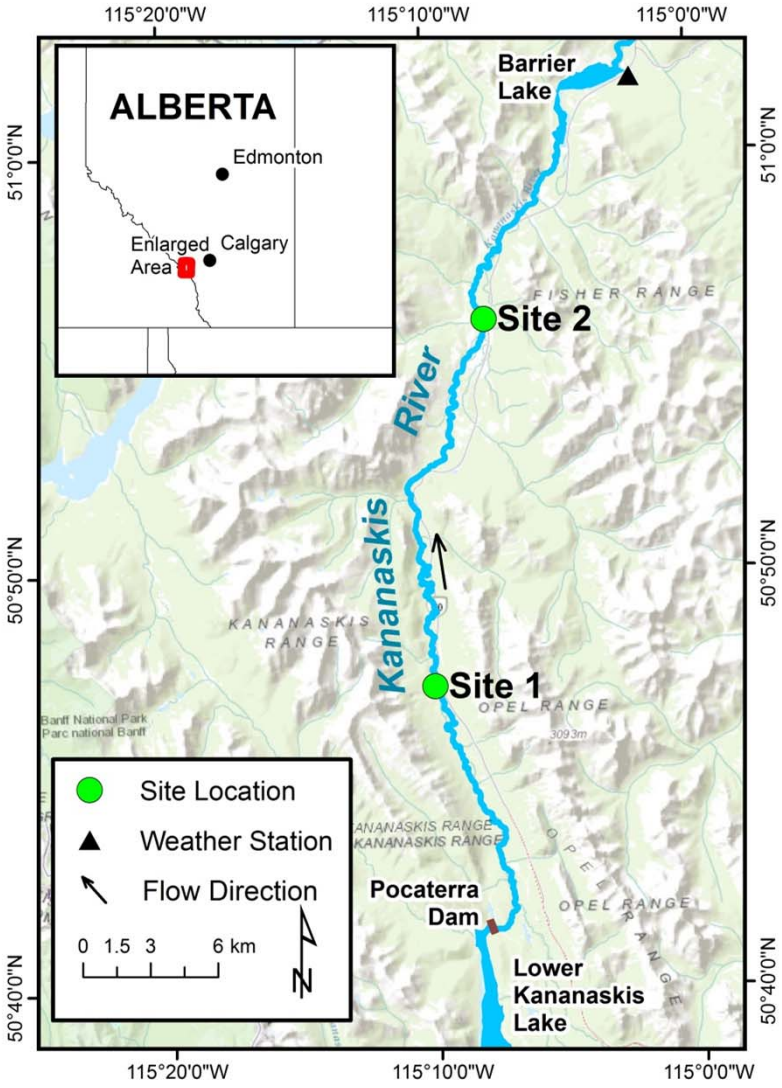

Figure 1. Location of study sites on the Kananaskis River, in Alberta, Canada.

a) b)

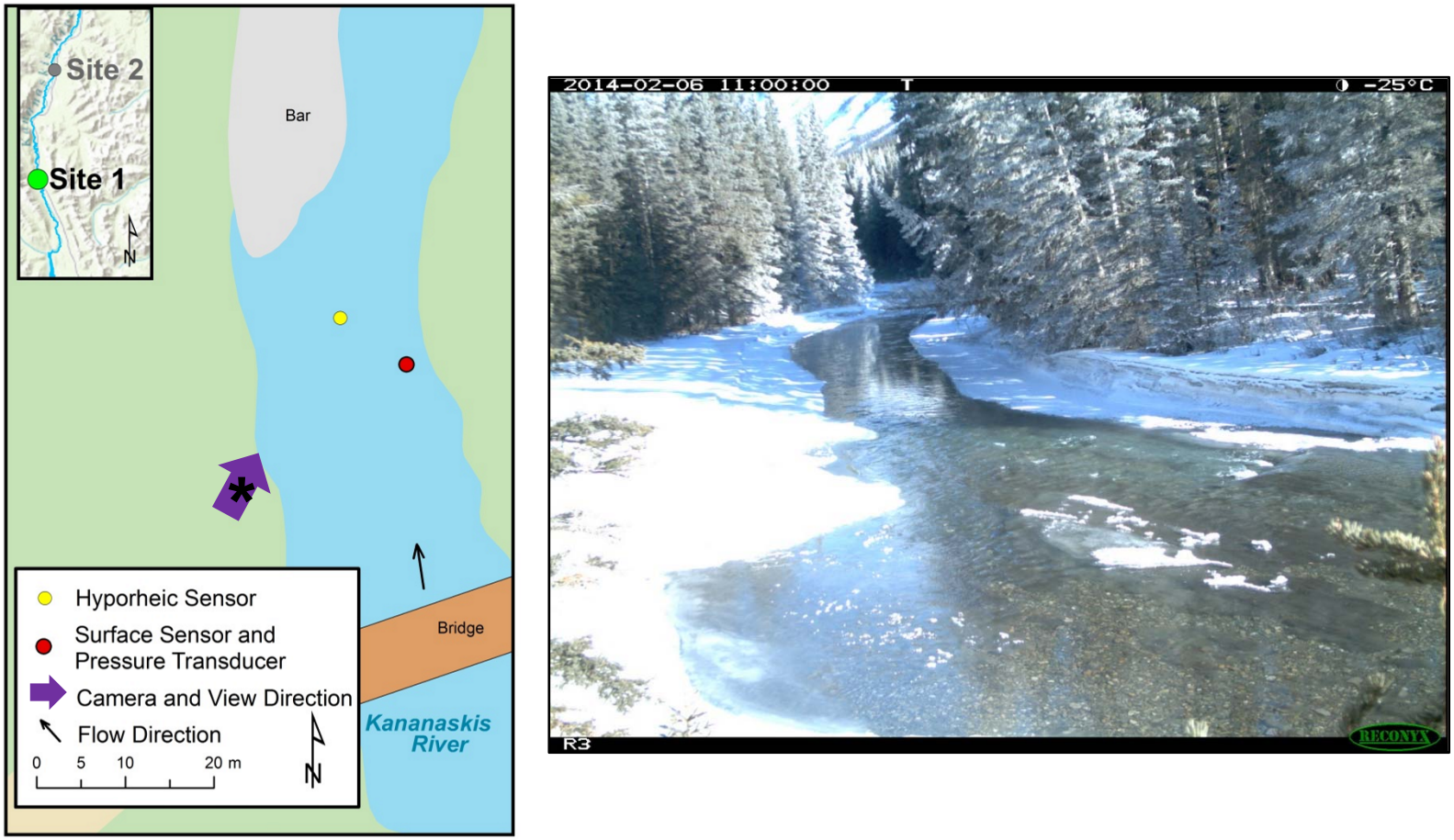

Figure 2. a) Location of instrumentation and b) typical ice conditions showing anchor ice at Site 1 on the Kananaskis River.

a) b)

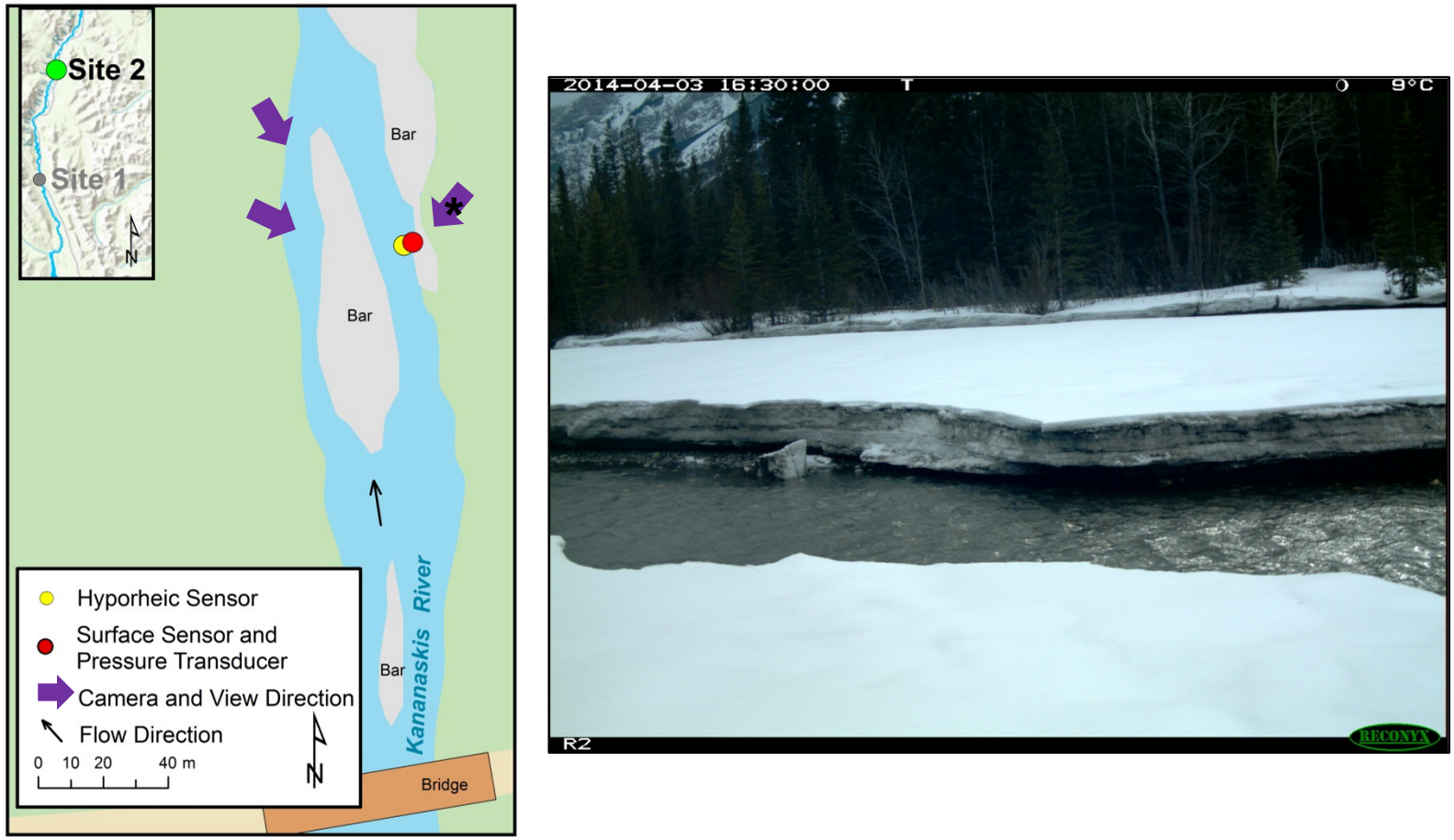

Figure 3. a) Location of instrumentation and b) typical ice conditions showing section view of exposed layered anchor ice after it had partially melted at Site 2 on the Kananaskis River.

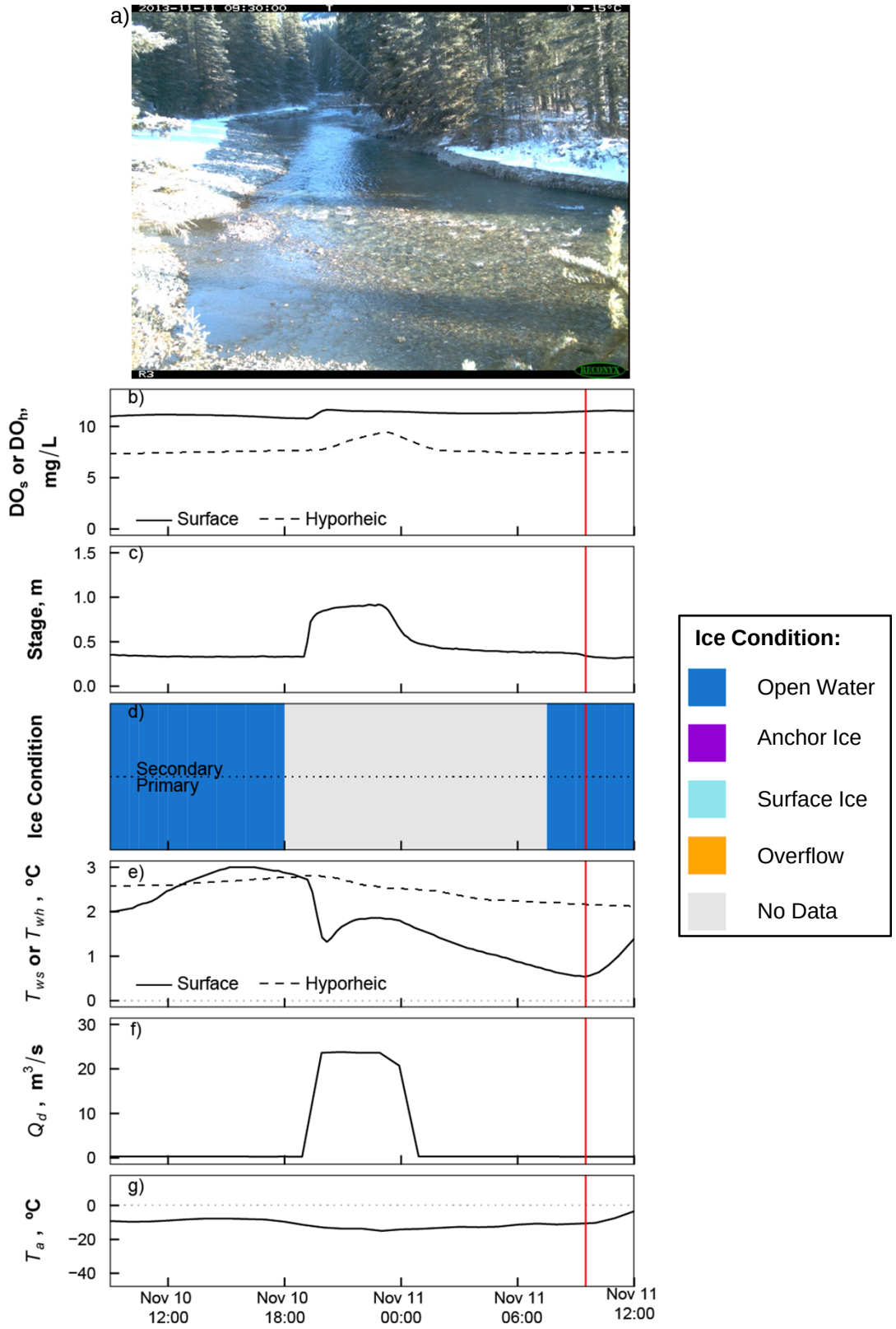

Figure 4. Measured parameters for Time Period 1 at Site 1 on the Kananaskis River. DO = dissolved oxygen (surface and hyporheic), T_w = water temperature (surface and hyporheic), Q_d = dam discharge lagged by travel time to site, T_a = air temperature, red vertical line is time of photo in a).

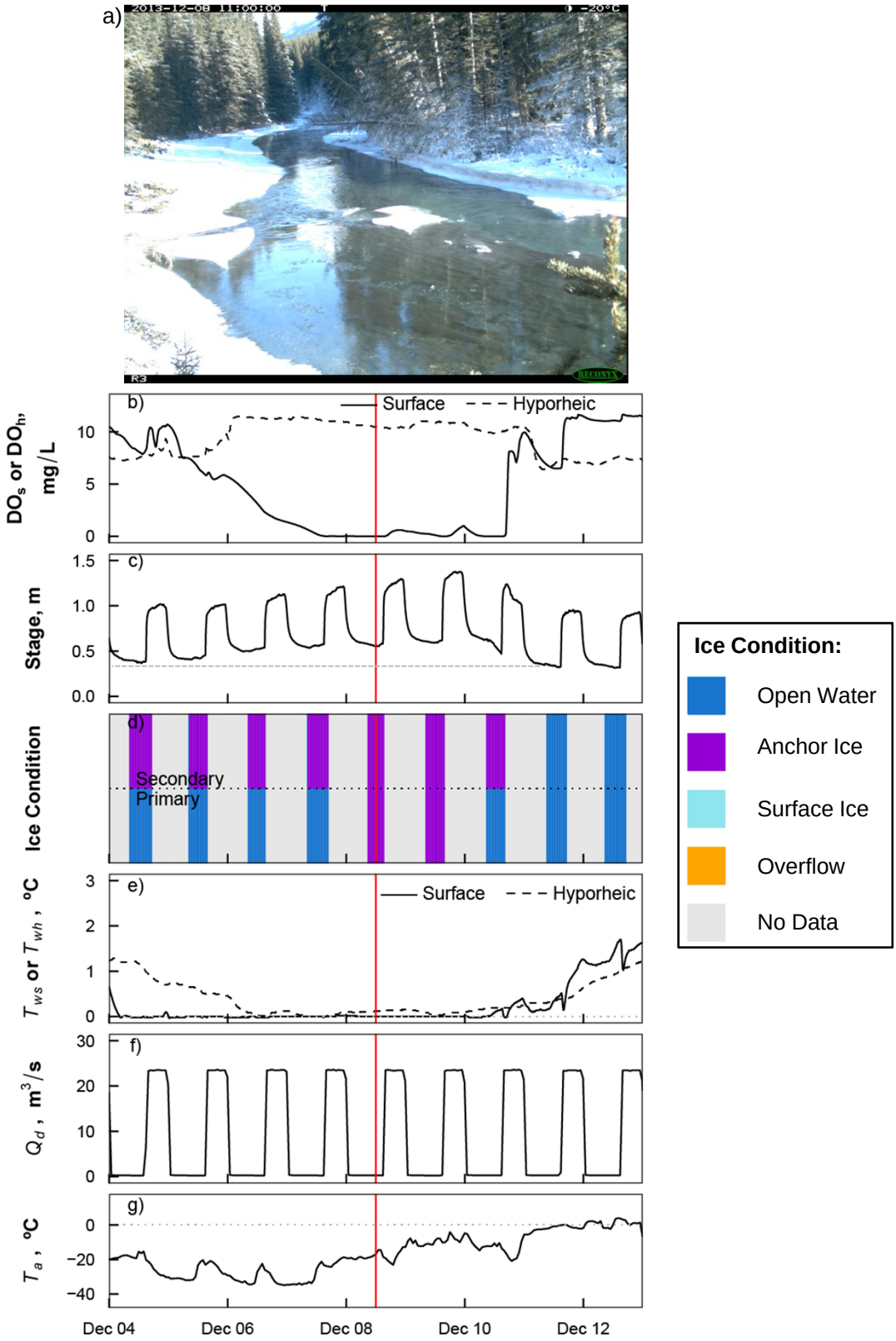

Figure 5. Measured parameters for Time Period 2 at Site 1 on the Kananaskis River. DO = dissolved oxygen (surface and hyporheic), T_w = water temperature (surface and hyporheic), Q_d = dam discharge lagged by travel time to site, T_a = air temperature, red vertical line is time of photo in a). Horizontal dashed line in c) indicates ice-free low stage.

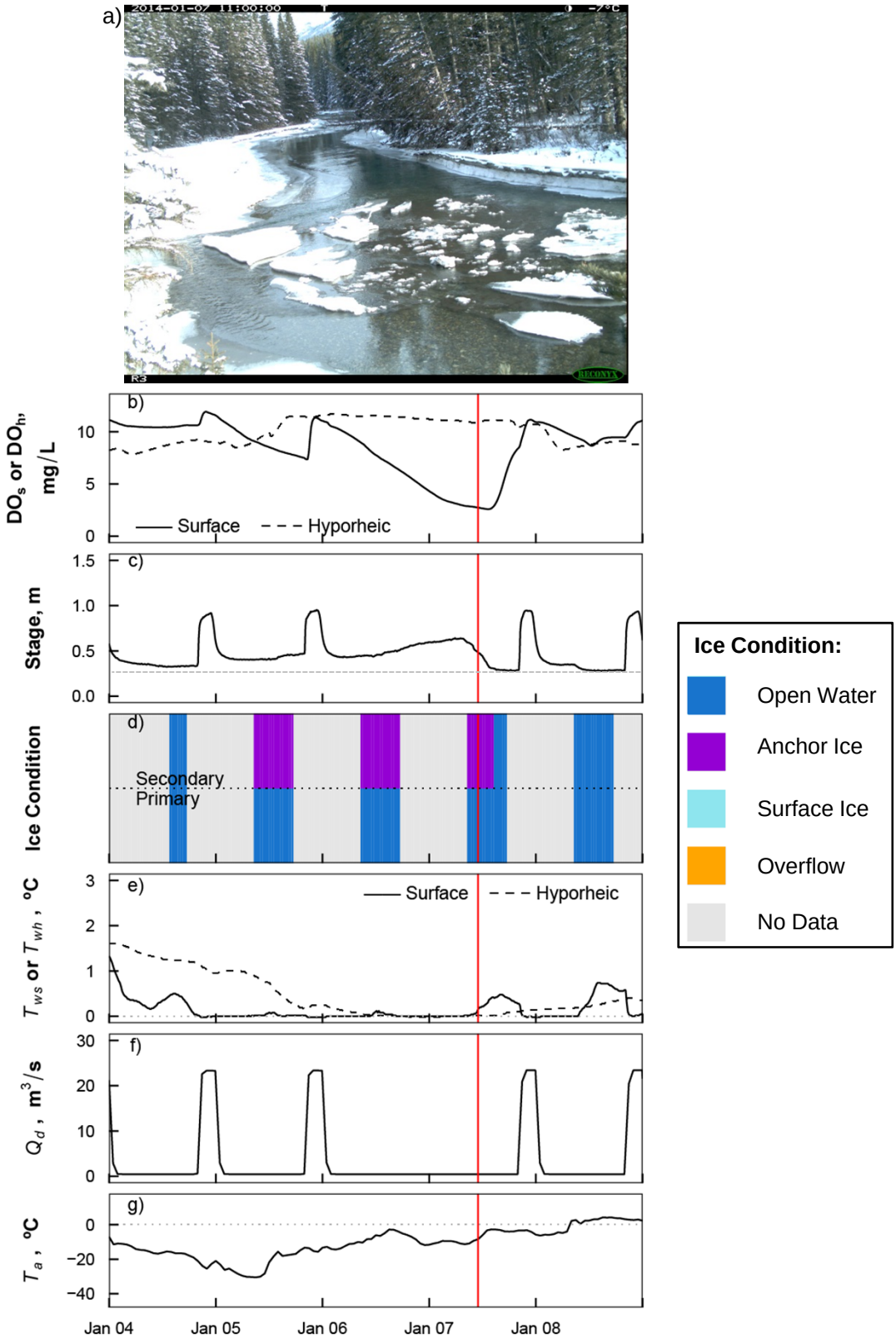

Figure 6. Measured parameters for Time Period 3 at Site 1 on the Kananaskis River. DO = dissolved oxygen (surface and hyporheic), T_w = water temperature (surface and hyporheic), Q_d = dam discharge lagged by travel time to site, T_a = air temperature, red vertical line is time of photo in a). Horizontal dashed line in c) indicates ice-free low stage.

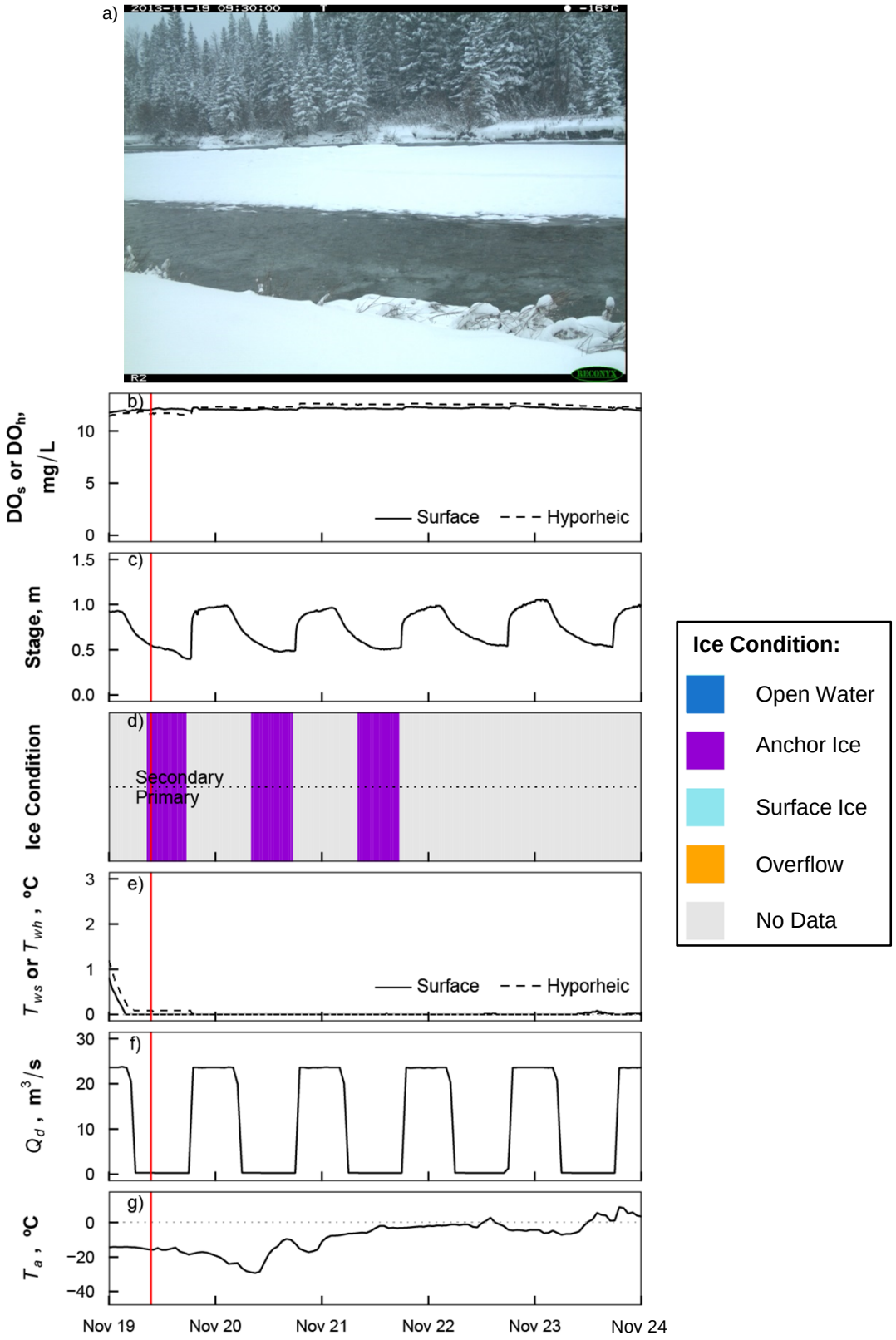

Figure 7. Measured parameters for Time Period 4 at Site 2 on the Kananaskis River. DO = dissolved oxygen (surface and hyporheic), T_w = water temperature (surface and hyporheic), Q_d = dam discharge lagged by travel time to site, T_a = air temperature, red vertical line is time of photo in a).

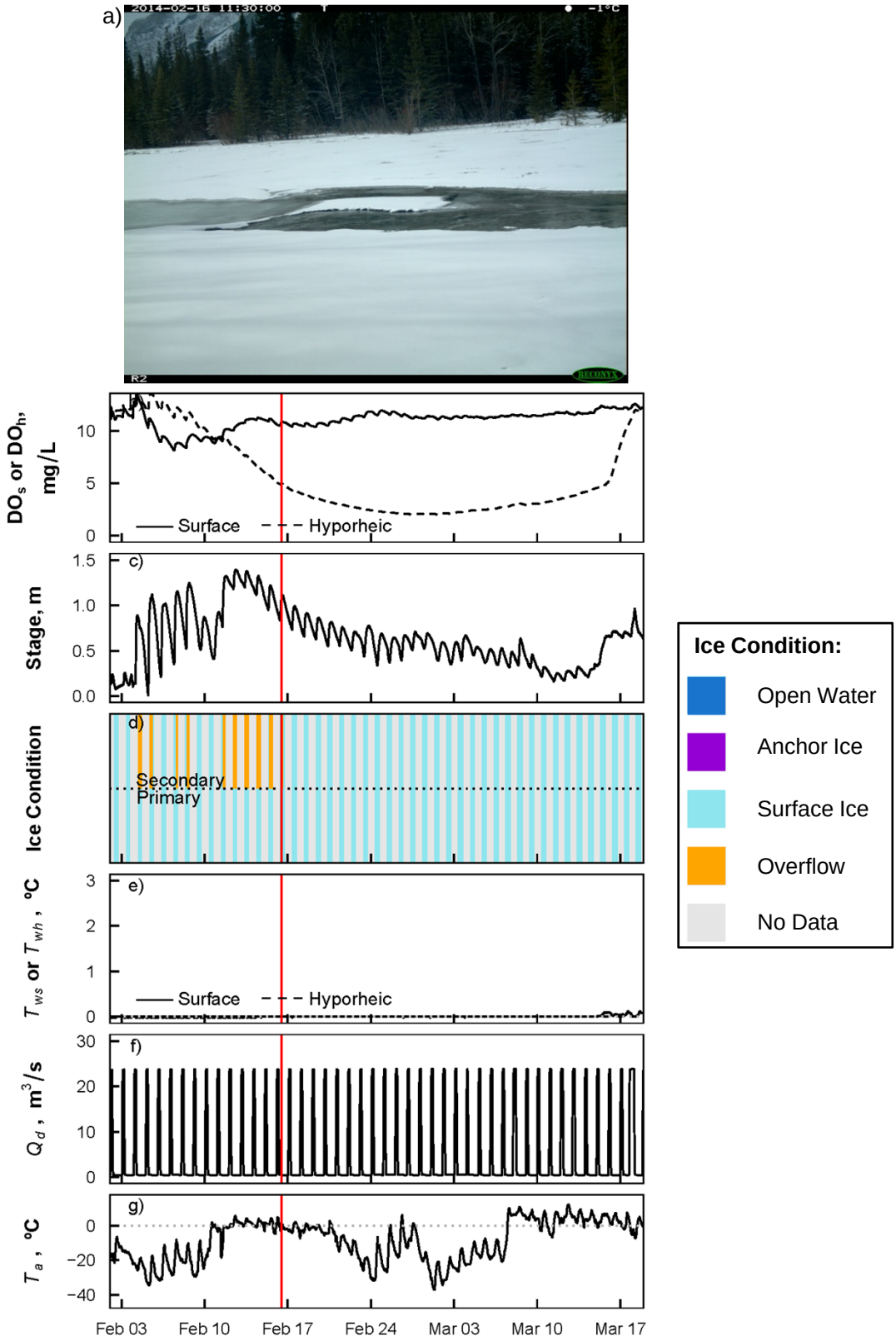

Figure 8. Measured parameters for Time Period 5 at Site 2 on the Kananaskis River. DO = dissolved oxygen (surface and hyporheic), T_w = water temperature (surface and hyporheic), Q_d = dam discharge lagged by travel time to site, T_a = air temperature, red vertical line is time of photo in a).

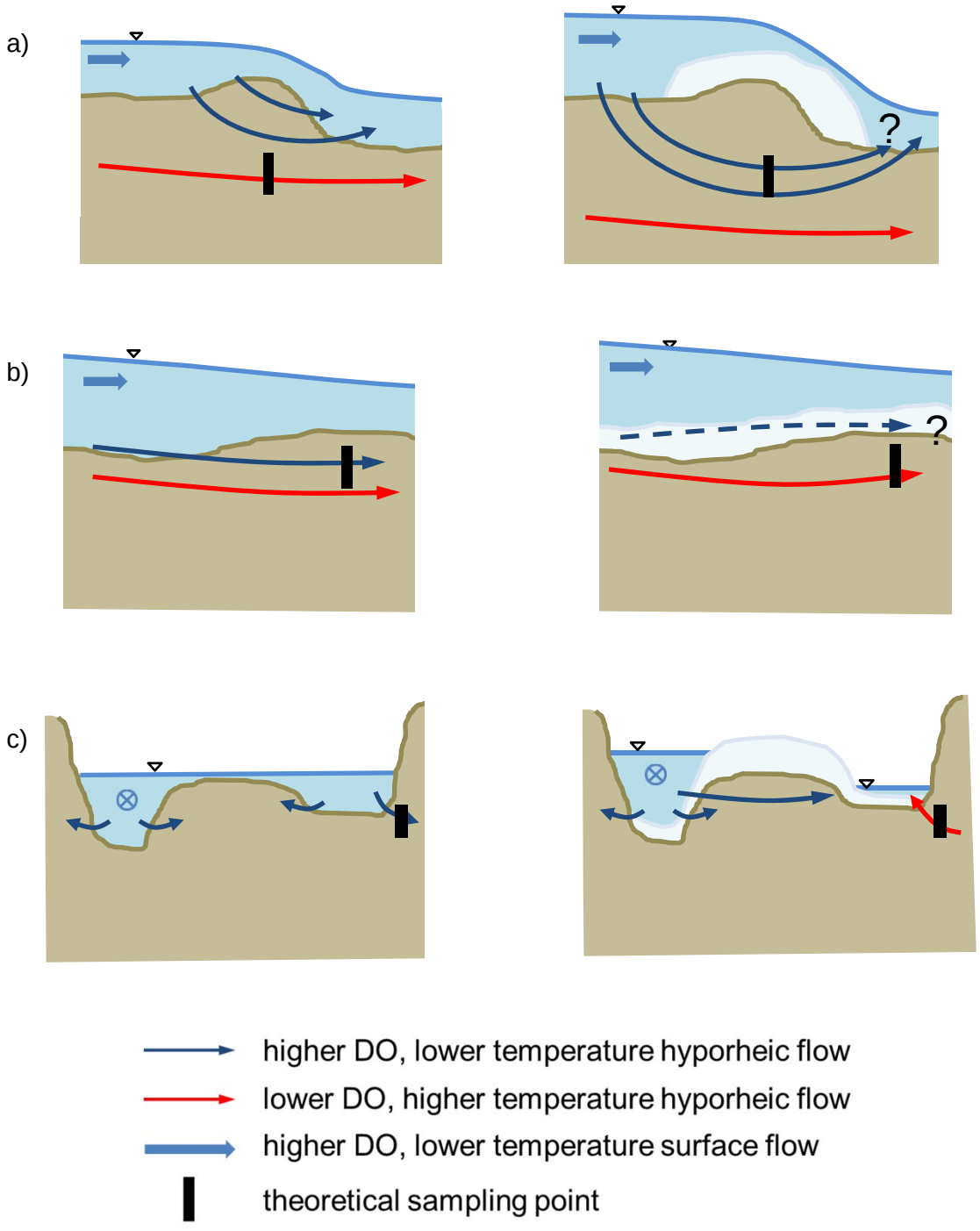

Figure 9. Possible theoretical hyporheic flow paths before (left panel) and during (right panel) anchor ice formation including: a) profile view of weir-like anchor ice accumulation at a riffle, b) profile view of carpet-like anchor ice accumulation, b) cross-section view of anchor ice at low flow with a bar, ⊗ = flow in into the page.